Could we observe Ultra High Energy Cosmic Rays from NGC1275?

N. Fraija[1]

Instituto de Astronomía, UNAM, México, 04510

Instituto de Física, UNAM, México, 04510

nifraija@astro.unam.mx

Received _____; accepted _____

[1]Instituto de Astronomía, Universidad Nacional Autónoma de México, Circuito Exterior, C.U., A. Postal 70-264, 04510 México D.F., México

ABSTRACT

Subject headings: Galaxies: active – Galaxies: individual (Centaurus A) – High energy cosmic ray: UHECR — radiation mechanism: nonthermal

1. Introduction

NGC 1275, also known as Perseus A and 3C 84, is the nearby active galaxy located at the centre of the Perseus cluster at redshift of $z = 0.0179$. This source has a strong, compact nucleus which has been studied in detail with very long baseline interferometry (VLBI)(Vermeulen et al. 1994; Taylor et al. 2006; Walker et al. 2000; Asada et al. 2006). These observations reveal a compact core and a bowshock-like souther jet component moving steadily outwards at 0.3 mas/year (Kellermann et al. 2004; Lister et al. 2009). The norther counter jet is also detected, though it is much less prominent due to Doppler dimming, as well as to free-free absorption due an intervening disk. Walker, Romney and Berson (1994) derive from these observations that the jet has an intrinsic velocity of $0.3c - 0.5c$ oriented at an angle $\approx 30°$ - $55°$ to the line of sight. Polarization has recently been detected in the southern jet(Taylor et al. 2006), suggesting increasingly strong interactions of the jet with the surrounding environment(**?**).

Perseus furthermore hosts a luminous radio mini halo - a diffuse synchrotron emission that fills a large fraction of the cluster core region - and shows a source extension of ≈200 kpc (Pedlar et al. 1990). This radio mini-halo is well modeled by the hadronic scenario where the radio emitting electrons are produced in hadronic CR proton interaction with ambient gas protons requiring only a very modest fraction of few percent CR pressure relative to thermal pressure (Pfrommer & Enblin 2004). These conditions provide high target densities for hadronic CRp-p interactions and enhance the resulting γ-ray flux (**?**). This source has been detected by MAGIC telescopes with a statistical significance of $6.6\,\sigma$ above 100 GeV in 46 hr of stereo observations carried out between August 2010 and February 2011. The measured differential energy spectrum between 70 GeV and 500 GeV can be described by a power law with a steep spectral index of $\Gamma = -4.1 \pm 0.7_{stat} \pm 0.3_{syst}$, and the average flux above 100 GeV is $F_\gamma = 1.3 \pm 0.2_{stat} \pm 0.3_{syst} \times 10^{-11}\, cm^{-2}\, s^{-1}$ (Aleksic et al. 2012).

It has been proposed that astrophysical sources accelerating ultra high energy cosmic rays (UHECRs) also could produce high energy γ-rays by proton interactions with photons at the source and/or the surrounding radiation and matter. Hence, VHE photons detected from Cen A could be the result of hadronic interactions of cosmic rays accelerated by the jet with photons radiated inside the jet or protons in the lobes (29; 52; 44; 45; 53; 40; 38; 3; 24).

Pierre Auger Observatory (PAO) studied the spectra of UHECR above 57 EeV through their shower properties finding a mixed composition of p and Fe (67; 2; 61). By contrast, HiRes data are consistent with a dominant proton composition at those energies, but uncertainties in the shower properties (61) and in the particle physics extrapolated to this extreme energy scale (26) preclude definitive statements about the composition. At least two events of the UHECRs observed by PAO were detected (1; 2) inside of a 3.1° circle centered at Cen A.

Synchrotron/Synchrotron-Self Compton (SSC) models have been very successful in explaining the multiwavelength emission from Broad-Line Lacertae (BL Lac) objects (18; 60). If FRIs are misaligned BL Lac objects, then one would expect synchrotron/SSC to explain their non-thermal spectral energy distribution (SED) as well. In the synchrotron/SSC scenario the low energy emission, radio through optical, originates from synchrotron radiation while high energy emission, X-rays through VHE γ-rays, originates from SSC. However, many blazars have higher energy synchrotron peaks, so this mechanism then covers much of the X-ray band; for them only the γ-rays come from SSC mechanism. In Cen A, synchrotron/SSC model has been applied successfully to fit the two main peaks of the SED, jointly or separated, with one or more electron populations (3; 22; 46; 50; 36). On the other hand, some authors (24; 33; 13) have considered hadronic processes to explain the VHE photons apparent in the SED.

In this work we use the fact that leptonic processes are insufficient to explain the

entire spectrum of NGC1275, and introduce hadronic processes that may leave a signature in the number of UHECRs observed on Earth. Our contribution is to describe jointly the SED of NGC1275 as well as the observed number of UHECR by PAO. We first require a description of the SED up to the highest energies obtaining parameters as: proton spectral index (α_p), proton proportionality constant (A_p) and the normalization energy (E_0). Then, we use these parameters to estimate the expected UHECRs observed by PAO. The main assumption here, is the continuation of the proton spectrum to ultra high energies. We also estimate the neutrino expectation in a hypothetical Km^3 telescope when considering that the VHE photons in the SED of Cen A are produced by pp interaction.

2. Jet Dynamics

HERE I HAVE TO DESCRIBE OPTICAL DEPTH, EMISSION REGION, ETC

3. Hadronic Model

Some authors (49; 16; 57; 25) have considered possible different mechanisms where protons up to ultra high energies can be accelerated. Thus, we suppose that Cen A is capable of accelerating protons up to ultra high energies with a power law injection spectrum (33),

$$\frac{dN_p}{dE_p} = A_p \, E_p^{-\alpha_p} \tag{1}$$

where α_p is the proton spectral index and A_p is the proportionality constant. Energetic protons in the jet mainly lose energy by pγ and pp interactions (58; 14; 13; 7; 25); as described in the following subsections.

3.1. pγ interaction

The pγ; interaction takes place when accelerated protons collide with target photons. The single-pion production channels are $p + \gamma \rightarrow n + \pi^+$ and $p + \gamma \rightarrow p + \pi^0$, where the relevant pion decay chains are $\pi^0 \rightarrow 2\gamma$, $\pi^+ \rightarrow \mu^+ + \nu_\mu \rightarrow e^+ + \nu_e + \bar{\nu}_\mu + \nu_\mu$ and $\pi^- \rightarrow \mu^- + \bar{\nu}_\mu \rightarrow e^- + \bar{\nu}_e + \nu_\mu + \bar{\nu}_\mu$ (7).

In this analysis we suppose that protons interact with SSC photons (~ 150 keV) in the same knot. If so, the optical depth is given as $\tau_{p,ssc} \approx r_d\, \theta_{jet}\, \Gamma\, n^{obs}_{\gamma ssc} \sigma_{p\gamma}$, where r_d is the value of the dissipation radius (15), θ_{jet} is the jet aperture angle, $\sigma_{p\gamma} = 0.9$ mbarn is the cross section for the production of the delta-resonance in proton-photon interactions and $n^{obs}_{\gamma ssc}$ is the particle density of SSC photons into the observer frame (13) given by,

$$n^{obs}_{\gamma ssc} \approx \frac{\epsilon_{knot}\, L^{obs}}{4\pi\, r_d^2\, E^{obs}_{\gamma,c}} \tag{2}$$

Assuming that the luminosity of a knot along the jet is a fraction $\epsilon_{knot} \approx 0.1$ of the observed luminosity $L^{obs} = 5 \times 10^{43}\, erg\, s^{-1}$ for $E^{obs}_{\gamma,c}$ keV, the optical depth is,

$$\tau_{p,ssc} \approx\ \Gamma^{-1} \left(\frac{\theta_{\rm jet}}{0.3}\right) \left(\frac{\epsilon_{\rm knot}}{0.1}\right) \left(\frac{L^{obs}}{6 \times 10^{43}\,{\rm erg\,s^{-1}}}\right) \left(\frac{r_d}{10^{16}\,{\rm cm}}\right)^{-1} \left(\frac{E^{obs}_{\gamma,b}}{\rm keV}\right)^{-1}. \tag{3}$$

The energy lost rate due to pion production is (58; 14),

$$t'_{p,\gamma} = \frac{1}{2\,\gamma_p} \int_{\epsilon_0}^{\infty} d\epsilon\, \delta_\pi(\epsilon) \xi(\epsilon)\, \epsilon \int_{\epsilon/2\gamma_p}^{\infty} dx\, x^{-2}\, n(x) \tag{4}$$

where $n(x) = dn_\gamma / d\epsilon_\gamma(\epsilon_\gamma = x)$, $\sigma_\pi(\epsilon)$ is the cross section of pion production for a photon with energy ϵ in the proton rest frame, $\xi(\epsilon)$ is the average fraction of energy transferred to the pion, and $\epsilon_0 = 0.15$ is the threshold energy, $\gamma_p = \epsilon_p / m_p^2$.

The rate of energy loss, $t'_{p,\gamma}$, $f_{\pi^0,p\gamma} \approx t'_d/t'_{p,\gamma}$ (where $t'_d \sim r_d/\Gamma$ is the expansion time scale), can be calculated by following Waxman & Bahcall 1997 formalism.

$$f_{\pi^0,p\gamma} \approx \frac{(1+z)^2\, L^{obs}}{8\,\pi\,\Gamma^2\,\delta_D^2\,dt^{obs}\,E^{obs}_{\gamma,b}}\sigma_{\epsilon_{peak}}\,\xi(\epsilon_{peak})\,\frac{\Delta\epsilon_{peak}}{\epsilon_{peak}}\begin{cases}\frac{E_p^{obs}}{E_{p,b}^{obs}} & E_p^{obs} < E_{p,b}^{obs}\\ 1 & E_p^{obs} \geq E_{p,b}^{obs}\end{cases} \tag{5}$$

Here, $\sigma_{peak} \approx 5 \times 10^{-28}$ cm^2 and $\xi(\epsilon_{peak}) \approx 0.2$ are the values of σ and ξ at $E_\gamma \approx \epsilon_{peak}$ and $\Delta\epsilon_{peak} \approx 0.2$ GeV is the peak width.

The differential spectrum, dN_γ/dE_γ of the photon-pions produced by pγ interaction is related to the fraction of energy lost through the equation: $f_{\pi^0}(E_p)\,E_p\,dN_p/dE_p\,dE_p = E_\gamma\,dN_\gamma/dE_\gamma\,dE_\gamma$. If we take into account that π^0 typically carries 20% of the proton's energy and that each produced photon shares the same energy then, we obtain the observed gamma spectrum through the following relationship,

$$\left(E^2\,\frac{dN}{dE}\right)^{obs}_{\pi^0-p\gamma} = A_{p,\gamma}\begin{cases}\left(\frac{E_\gamma^{obs}}{E_0}\right)^{-1}\left(\frac{E_{\gamma,c}^{obs}}{E_0}\right)^{-\alpha_p+3} & E_\gamma^{obs} < E^{obs}_{\pi^0-\gamma,c}\\ \left(\frac{E_\gamma^{obs}}{E_0}\right)^{-\alpha_p+2} & E^{obs}_{\pi^0-\gamma,c} < E_\gamma^{obs}\end{cases} \tag{6}$$

where

$$A_{p,\gamma} = 2.25{\times}10^{-13}\frac{\delta_D^{\alpha_p}\,E_0^2\,A_p\,(11s.1)^{2-\alpha_p}e^{-\tau_{\gamma\gamma}}}{(1+z)^\alpha}\left(\frac{E^{obs}_{\gamma,c}}{\mathrm{keV}}\right)^{-1}\left(\frac{L^{obs}}{6\times10^{43}\,\mathrm{erg\,s^{-1}}}\right)\left(\frac{dt^{obs}}{3.17\times10^7 s}\right)\left(\frac{d_z}{76\,\mathrm{Mpc}}\right)^{-2} \tag{7}$$

and

$$E^{obs}_{\pi^0-\gamma,c} = \mathrm{GeV}\frac{\delta_{\mathrm{D}}^2}{(1+\mathrm{z})^2}\left(\frac{\mathrm{E}^{\mathrm{obs}}_{\gamma,\mathrm{b}}}{\mathrm{keV}}\right)^{-1} \tag{8}$$

The eq. 6 could represent the VHE photon contribution to the spectrum.

3.2. PP interaction

Hardcastle et al. 2009 argues that the number density of thermal particles within the giants lobes is $n_p \sim 10^{-4}\, cm^{-3}$. If we assume that the accelerated protons collide with this thermal particle target then, the energy lost rate due to pion production is given by (7),

$$t'_{pp} = (n'_p\, k_{pp}\, \sigma_{pp})^{-1} \tag{9}$$

where $\sigma_{pp} = 30$ mbarn is the nuclear interaction cross section, $k_{pp} = 0.5$ is the inelasticity coefficient and n'_p is the comoving thermal particle density. The fraction of energy lost by pp is $f_{\pi^0,pp} \approx t'_d/t'_{pp}$ then,

$$f_{\pi^0,pp} = R\, n'_p\, k_{pp}\, \sigma_{pp} \tag{10}$$

where R is the distance to the lobes from the AGN core.

The differential spectrum, dN_γ/dE_γ of the photon-pions produced by pp interaction is related to the fraction of energy lost through the equation: $f_{\pi^0,pp}(E_p)\, E_p\, (\frac{dN_p}{dE_p})\, dE_p = E_\gamma\, (\frac{dN_\gamma}{dE_\gamma})\, dE_\gamma$. Taking into account that photon carries 18% of the proton energy, we have that the observed pp spectrum is given by (33),

$$\left(E^2\, \frac{dN}{dE}\right)^{obs}_{\pi^0-pp} = A_{pp}\, \left(\frac{E^{obs}_\gamma}{E_0}\right)^{2-\alpha_p} \tag{11}$$

where,

$$A_{pp} = 9.97 \times 10^{-21} \frac{\Gamma^2\, \delta_D^2\, E_0^2\, A_p\, e^{-\tau_{\gamma\gamma}}}{(1+z)^2}\, R_{\rm kpc}\, n'_{p,{\rm cm}^{-3}}\, \left(\frac{dt^{obs}}{3.17 \times 10^7 s}\right)^2 \left(\frac{d_z}{76\,{\rm Mpc}}\right)^{-2} \tag{12}$$

The eq. 11 could represent the VHE photon contribution to the spectrum.

4. Calculation of physical parameters and expected UHECRs

A broadband fit to the SED of Cen A (data from Abdo et al. 2010) using our leptonic model (blue line) plus either pγ or pp emission is shown in Figures 1 and 2 respectively. For this fit, we have adopted typical values reported in the literature such as luminosity (L^{obs}), variability (dt^{obs}), thermal particle target density (n_p) and lobes distance (R)(3; 24; 36; 53). The viewing angle was chosen in accordance with the observed infrared range (see, e.g. 39, and reference therein). Then, from the fit we obtain the values of the bulk Lorentz factor (Γ), ratio of expansion time (f_{es}), proportionality constants (A_e, A_{ic}, $A_{p\gamma}/A_{pp}$), magnetic field parameter (ξ_B), electron parameters (ξ_e) and spectral index (α). Other quantities as magnetic field (B), electrons Lorentz factors ($\gamma_{e,min}$, $\gamma_{e,c}$), comoving radius (r_d), etc, are deduced these parameters. Table 1 shows all the values for used, obtained and deduced parameters in and from the fit.

The fit of the VHE photon spectrum with a hadronic model (either pγ or pp interaction) determines the spectral index α_p, energy normalization E_0 and proportionality constant A_p (see section 2). So, we calculate the number of UHECRs expected on Earth. Results are given in Table 1. As shown, the expected number of UHECRs is extremely high if we consider the VHE spectral gamma contribution to come from pγ interactions, while considering pp interactions the expected number of UHECRs is in agreement with PAO observations.

Name	Symbol	Value
Input parameters to the model		
Variability timescales (s)	dt^{obs}	2.5×10^6 (3)
Luminosity (erg s^{-1})	L^{obs}	5×10^{43} (3)
Jet angle (degrees)	θ	40 (39)
Normalization constant (leptonic process) (MeV)	E_0	0.1 (41)
Normalization constant (pγ process) (TeV)	E_0	1 (5)
Normalization constant (pp process) (TeV)	E_0	1 (5)
Thermal particle target density in lobes (cm^{-3})	n_p	1×10^4 (36)
Lobes distance (kpc)	R	100 (36)
Calculated parameters with the model		
Bulk Lorentz factor	Γ	2.06 ± 0.03
Electron spectral index	α	2.837 ± 0.004
Magnetic field parameter	ϵ_B	0.1073 ± 0.0008
Electron energy parameter	ϵ_e	0.79 ± 0.14
Ratio of expansion time	f_{es}	0.0385 ± 0.0003
Proportionality electron constant $(eVcm^2s)^{-1}$	A_e	$(4.368 \pm 0.003) \times 10^{15}$
Proportionality IC constant $(eVcm^2s)^{-1}$	A_{ic}	$(9.65 \pm 0.07) \times 10^{16}$
Proportionality proton constant $(TeVcm^2s)^{-1}$	A_{pp}	$(5.9 \pm 0.4) \times 10^{-7}$
Proportionality proton constant $(TeVcm^2s)^{-1}$	$A_{p\gamma}$	$(1.37 \pm 0.99) \times 10^4$
Proton spectral index	α_p	2.805 ± 0.008
Derived quantitatives		
Doppler factor	δ_d	1.47
Magnetic field (G)	B	0.19
Comoving radius (cm)	r_d	3.8×10^{16}
Minimum electron Lorentz factor	γ_m	1.36×10^3
Break electron Lorentz factor	γ_c	3.47×10^3
Apparent UHECR Luminosity (pγ) $(erg\,s^{-1})$	L_p	2.7×10^{49}
Apparent UHECR Luminosity (pp) $(erg\,s^{-1})$	L_p	2.9×10^{39}
Predicted number of events: pγ interaction	$N_{ev,p\gamma}$	8.371×10^{10}
Predicted number of events: pp interaction	$N_{ev,pp}$	2.29

Table 1. Parameters used and obtained from and in the fit of the spectrum of Centaurus A.

5. UHECRs from Cen A

The Pierre Auger Observatory, localized in the Mendoza Province of Argentina at $\approx 36^\circ$ S latitude, determines the arrival directions and energies of UHECRs using four fluorescence telescope arrays and 1600 surface detectors spaced 1.5 km. The large exposure of its ground array, combined with accurate energy and arrival direction measurements, calibrated and verified from the hybrid operation with the fluorescence detectors, provides an opportunity to explore the spatial correlation between cosmic rays and their sources in the sky. The Pierre Auger Collaboration reported an anisotropy in the arrival direction of UHECRs (1; 2). While a possible correlation with nearby AGNs is still under discussion, it has been pointed out that some of the events can possibly be associated with Cen A (e.g. 30; 47; 44).

The corrected PAO exposure for a point source is given by $\Xi\, t_{op}\, \omega(\delta_s)/\Omega_{60}$, where $\Xi\, t_{op} = (\frac{15}{4})\, 9 \times 10^3\, \mathrm{km}^2\, \mathrm{yr}$, t_{op} is the total operational time (from 1st January 2004 until August 31st, 2007), $\omega(\delta_s) \simeq 0.64$ is an exposure correction factor for the declination of Cen A, and $\Omega_{60} \simeq \pi$ is the Auger acceptance solid angle (23). For a proton power law with spectral index α_p and proportionality constant A_p, the expected number of UHECRs from Cen A observed by PAO above an energy, $\mathrm{E_{min}}$, is given by,

$$N_{UHECR} = \frac{\Xi\, t_{op}\, \omega(\delta_s)}{(\alpha - 1)\, \Omega_{60}}\, A_p\, E_0 \left(\frac{E_{min}}{E_0}\right)^{-\alpha_p + 1} \tag{13}$$

where E_0 is the normalization energy. In other words, the expected number of UHECRs depends on the proton spectrum parameters. If we assume that protons at lower energies have hadronic interactions responsible for producing the observed gamma-ray spectra at very high energies then we can estimate these parameters. An interesting quantity is the apparent isotropic UHECR luminosity that also depends on the spectrum parameters as,

$$L_p = \frac{4\,\pi\,d_z^2\,A_p\,E_0^2}{(\alpha_p - 2)}\,\left(\frac{E_{min}}{E_0}\right)^{2-\alpha_p} \tag{14}$$

where d_z is the distance to Cen A. On the other hand, during flaring intervals the apparent isotropic jet power can reach $\approx 10^{46}$erg s^{-1}, hence the maximum particle energies of a cold relativistic wind with velocity β, apparent isotropic luminosity (L), Lorentz factor (Γ) and equipartition parameter of the magnetic field (ϵ_B) is given by (24),

$$E_{max} \approx 3 \times 10^{20}\,\frac{\sqrt{\epsilon_B\,L/10^{46}\,erg\,s^{-1}}}{\beta^{3/2}\,\Gamma}\,eV \tag{15}$$

where $\Gamma = 1/\sqrt{1-\beta^2}$.

6. Neutrino expectation for Cen A

The principal neutrino emission processes in the AGNs are hadronic. These interactions produce both, high energy neutrinos and high energy gamma rays, through pionic decay. As we mentioned before, hadronic interactions generate mainly pions by $p + p \rightarrow \pi^0 + \pi^+ + \pi^- + X$ (where X is an hadronic product) and $p + \gamma \rightarrow \Delta^+ \rightarrow \pi^0 + \pi^+$. The resulting neutral pion decays into two gamma rays, $\pi_0 \rightarrow \gamma\gamma$, and the charged pion into leptons and neutrinos, $\pi^\pm \rightarrow e^\pm + \nu_\mu/\bar{\nu}_\mu + \bar{\nu}_\mu/\nu_\mu + \nu_e/\bar{\nu}_e$. The effect of neutrino oscillations on the expected flux balances the number of neutrinos per flavor (12) arriving at Earth. Therefore, the measured emission of high energy gamma rays from AGNs suggests the possibility to have an equivalent high-energy neutrino flux. In the case of Cen A the redshift is $z = 0.0018$, therefore VHE photons are not absorbed from EBL and we can consider the observed high energy gamma ray spectra as the intrinsic spectra emitted by this source and we can use it for the neutrino flux estimation.

Concerning the physics environment of Cen A, the optimistic conditions assumed to calculate the neutrino expectations are the following,

1. The high energy gamma ray flux detected by HESS are produced according to the pp hadronic scenario in Cen A.

2. The considered neutrino flux correlated to high energy gamma ray activity has a minimum duration of 1 year (i.e. the source is assumed to be stable).

3. The neutrino spectrum of Cen A is assumed without any cut-off.

4. The observed gamma-ray spectrum is considered as the intrinsic spectrum of Cen A.

Considering that neutrinos and gamma rays are produced by the same hadronic interaction (pp), we follow the description of Becker(2008) to correlate these two messengers and we assume the neutrino spectrum to be the same as the VHE gamma spectrum recorded by H.E.S.S. Therefore we perform a Monte Carlo simulation of a possible Km^3 neutrino telescope in the Mediterranean sea in order to calculate the expected neutrino event rate. We choose this location to have a good sensitivity with respect to the position of Cen A.

The Monte Carlo simulation takes into account the neutrino source position, the propagation of neutrino through water, the charged current interaction with the respective muon production, the Cherenkov light produced by the muon, the photons produced by the electromagnetic showers and the response of the simulated neutrino telescope. Then we calculate the signal to noise ratio in the telescope.

In this analysis the neutrino "backgrounds" are represented by atmospheric neutrinos and cosmic diffuse neutrinos. The atmospheric neutrino "background" is generated by the interaction of high energy cosmic rays with nuclei in the atmosphere. The cosmic diffuse neutrino "background" is taken as the average rate of neutrinos generated by

all the galactic and extragalactic non-resolved sources. This cosmic diffuse neutrino flux is discussed by Waxman and Bahcall (9; 65) and his upper limit is given as $E_\nu^2\, d\Phi/dE_\nu < 4.5 \times 10^{-8} GeV cm^{-2} s^{-1} sr^{-1}$. The atmospheric neutrino flux implemented in our Monte Carlo is well described by the Bartol model (10; 11) in the range between 10 GeV and 100 TeV. We do not consider the "background" from atmospheric muon flux since it is filtered out by the Earth because Cen A is most of the time under the horizon for our hypothetical telescope, see Fig.**??**. For the calculation of signal to noise ratio we take into account only the "background" inside the portion of the sky covered by a cone centered in the Cen A position and having an opening angle of 1° . This selection is motivated by the angular resolution of our neutrino telescope.

Using the assumed neutrino spectrum we obtain for the Km^3 telescope the expected neutrino event rate shown in Fig. **??**. As observed, the integrated signal neutrino event rate in one year of recording data is one order of magnitude below the cosmic neutrino event rate and two order of magnitude below the atmospheric neutrino event rate reconstructed in the region around Cen A. Moreover, even considering few years of neutrino telescope operation, with the considered spectrum, we are not able to disentangle neutrino emission from Cen A.

7. Summary and conclusions

We have presented a leptonic and hadronic model to describe the broadband photon spectrum of Cen A. Our model has eight free parameters (equipartition magnetic field, equipartition electron energy, bulk Lorentz factor, spectral index, ratio of expansion time and proportionality constants). The leptonic model describes the spectrum up to a few GeV energies while the hadronic model describes the Cen A spectrum at TeV energies. Two hadronic interactions have been considered, $p\gamma$ and pp interactions. In the first case, the

target is considered as SSC photons with energy of ~ 150 keV, while in the second case, the target protons are those in the lobes of Cen A. Only one hadronic interaction is considered at the time but in both cases, the proton spectrum is extrapolated up to ultra high energies to estimate the number of UHECR events expected at Earth. We have required a good description of the photon spectrum to obtain values for the quantities required to estimate the UHECR events.

When pγ interaction is considered, the expected number of UHECR obtained is several orders of magnitude above the observed by PAO. However, when pp interaction is considered, the expected number of UHECR is in very good agreement with PAO observations.

We have also calculated the neutrino event rate from pp interactions observed by a hypothetical Km^3 neutrino telescope in the Mediterranean sea. We have calculated the signal to noise ratio considering atmospheric and cosmic neutrino "backgrounds". We have obtained that the expected signal event rate is below the required one to disentangle the neutrino emission from Cen A from the "backgrounds".

We thank the anonymous referee for the comments given to improve the paper. We also thank to Charles Dermer, Markus Bötcher, Parisa Roustazadeh, Bin Zhang, Giulia DeBonis, Bachir Bouhadef, Mauro Morganti, Dario Grasso, Antonio Stamerra and Teresa Montaruli for useful discussions.

This work was supported by DGAPA-UNAM (Mexico) Project Numbers IN112910 and IN105211 and Conacyt project number 105033.

REFERENCES

Abraham J. et al. (Pierre Auger Collaboration), 2007, Science, 318, 938

Abraham J. et al. (Pierre Auger Collaboration), 2008, ApJ, 29, 198.

Abdo A. A. et al. (FERMI Collaboration), 2010, ApJ, 719, 1433.

Aharonian F. et al. (HESS Collaboration), 2005, A&A, 441, 465.

Aharonian F. et al. (HESS Collaboration), 2009, ApJ, 695, L40.

Allen W.H. et al. (JANZOS Collaboration), 1993, ApJ, 405, 554.

Atoyan A. M & Dermer C. D., 2003, ApJ, 589, 79.

Baity W. A. et al., 1981, ApJ244, 429.

Bahcall J. & Waxman E., 2001, Physical Review D., 64(2): 023002.

Barr G.D., Gaisser T. K. , Lipari P., Robbins S. & Stanev T., Phys. Rev. D 70, 023006 (2004).

Barr G.D., Gaisser T. K., Robbins S., & Stanev T., Phys. Rev. D 74, 094009 (2006).

Becker J. K., 2008, Physics Reports, 458 , 173.

Becker J. K. & Biermann P. L., 2009, Astropart. Phys. 31, 138.

Berezinskii, V.S., Bulanov S. V., Dogiel V. A., Ginzburg V. I. & Ptuskin V. S. 1990, Astrophysics pf Cosmic Rays (North-Holland:Amsterdam), Ch. 4.

Bhattacharjee P. & Gupta N., 2003, Astropart. Phys., 20, 169.

Bhattacharjee P. & Sigl G., 2000, Phys. Rept., 327, 109.

Blandford R. D. & McKee C. F., 1976, Phys. Fluids. 19, 1130.

Bloom, S. D. & Marscher, A. P. 1996, ApJ, 461, 657.

Bowyer C. S., Lampton M., Mack J. & De Mendonca F., 1970, ApJ161 L1.

Carramiñana et al., 1990, A&A, 228, 327.

Cheng K. S. & Wei D. M. 1996, MNRAS, 283, L133.

Chiaberge M., Capetti A. & Celotti 2001, MNRAS, 324, L33.

Cuoco A. & Hannestad S., 2008, Phys. Rev. D, 78, 023007.

Dermer C. D., Razzaque S., Finke J. D. & Atoyan A., 2009, New J. Phys. 11, 065016.

Dermer C. D. & Menon G. 2009, High energy radiation from Black Holes, Princeton University Press. 2009.

Engel R.l R (The Pierre Auger Collaboration), 2007, arXiv: 0706.1921.

Fragile P. C., Mathews G., Poirier J. & Totani T., 2004, Astropart. Phys. 20, 591.

Gallant Y. A., 2002, Lectures Notes in Physics, 589, 24.

Gopal-Krishna, Biermann P. L. , De Souza V. & Wiitta P. J., 2010, Astropart. Phys. 720, L155.

Gorbunov D., Tinyakov, P. Tkachev, I & Troitsky, S., 2008, Sov. J. Exp. Theor. Phys. Lett, 87, 461.

Grindlay J. E, Helmken H. F., Brown R. H.,Davis, J. & Allen L. R., 1975, ApJ, 197, L9.

Gupta N. & Zhang B. 2007, MNRAS, 380, 78.

Gupta N., 2008, JCAP, 7060806, 022.

Hague J. D.,(Pierre Auger Collaboration), 2009, Proc. 31st ICRC, Lodz

Hardcastle M. J., Worrall D. M., Kraft R. P., Forman W. R., Jones C. & Murray S. S., 2003, ApJ, 593, 169.

Hardcastle M. J., Cheung C. C., Feain I. J. & Stawarz L., 2009, MNRAS, 393, 1041.

Hinshaw et al., 2009, ApJS, 180, 225.

Honda M., 2009, ApJ, 706, 1517.

Horiuchi S., Meier D. L., Preston R. A. & Tingay S. J., 2006, PASJ, 58, 211.

Isola, C., Lemoine M. & Sigl G., 2002, Phys. Rev. D, 65, 023004.

Junkes E. et al., 1993, ApJ, 412, 586.

Junkes N., Haynes, R. F., Harnett, J.I., & Jauncy, D. L. 1993, A&A, 269,29.

Kabuki, S. et al. (CANGAROO III Colaboration) 2007, ApJ, 668, 968.

Kachelriess M., Ostapchenko S. & Tomas R., 2009, New J. Phys. 11, 065017.

Kachelriess M., Ostapchenko S. & Tomas R., 2009, Int. J. Mod. Phys. D 18, 1591.

Lenain J. P., Boisson C., Sol H. & Katarzynski K., 2008 A&A478, 111.

Moskalenko, I. V., Stawarz, L., Porter T. A. & Cheung, C. C., 2009, ApJ, 693, 1261.

Mushotzky R. F., Baity W. A., Wheaton W.A., & Peterson L. E., 1976 , ApJ, 206, L45.

Olinto A. V., 2000, Phys. Rept. 333, 329.

Orellana M. & Romero G. E., 2009 AIP Conf. Proc., 1123, 242.

Raue M. & Mazin D. , 2008, International Journal of Modern Physics 17, 1515.

Rieger F. M. & Aharonian F. A., 2009, A&A, 506, L41.

Romero G. E., Combi J. A., Anchordoqui L.A. & Perez S. E., 2009, Astropart. Phys., 5, 279.

Rowell, G. P. et al. (CANGAROO III Colaboration) 1999, Astropart. Phys. 11, 217.

Rybicki G.B. & Lightman A.P.1979, Radiative processes in Astrophysics (Wiley, New York. 1979).

Sreekumar P., Bertsch D. L., Hartman R. C., Nolan P.L. & Thompson D. J., 1999, ApJ, 11, 221.

Stanev T., 2004, High Energy Cosmic Rays, Springer, 2004.

Stecker F. W. 1968, Phys. Rev. Lett., 21, 1016.

Steinle H. et al., 1998, A&A, 330, 97.

Tavecchio, F., Maraschi, L. & Ghisellini, G., 1998, ApJ, 509, 608.

Unger M., Engel R., Schussler F., Ulrich R. & Pierre Auger Collaboration, 2007, Astron. Nachrichten, 328, 614.

Unger M., Dawson B.R., Engel R., Schussler F. & Ulrich R., 2008, Nucl. Instrum. Methods Phys. Res. A, 588, 433.

Vietri M., 1995 ApJ, 453, 883.

Waxman E. & Bahcall J., 1997, Phys. Rev. Lett. 78, 12.

Waxman E. & Bahcall J., 1998, Texas simposium on Relativistic Astrophysics and Cosmology, December 1998.

Winkler F. P. & White A. E. 1975 ApJ, 199, L139.

Yamamoto T. & Pierre Auger Collaboration, 2007, arXiv:0707.2638.

Vermeulen R.C., Readhead, A.C. & Backer D. C., 1994, ApJ, 430, L41.

Taylor et al., 2006, MNRAS, 368, 1500.

Walker R. C., Dhawan V., Rommey J.D., Kellermann K. I. & Vermeulen R. C., 2000 ApJ, 530, 233.

Asada K, et al. 2006, PASJ, 58, 261.

Kellermann K. I. et al. 2004, ApJ609, 539.

Lister et al., 2009, AJ 137, 3718.

Walker R. C., Dhawan V., Rommey J.D., Kellermann K. I. & Vermeulen R. C., 2000 ApJ, 530, 233.

Abdo A. A.et al. (FERMI Collaboration), 2009, ApJ, 707, 55

Pedlar, A., et al., 1990, MNRAS, 246, 477

Pfrommer, C., & Enlin, T. A. 2004a, A&A, 413, 17

Aleksic J. et al. (MAGIC Collaboration), 2012, A&A, 539, L2.

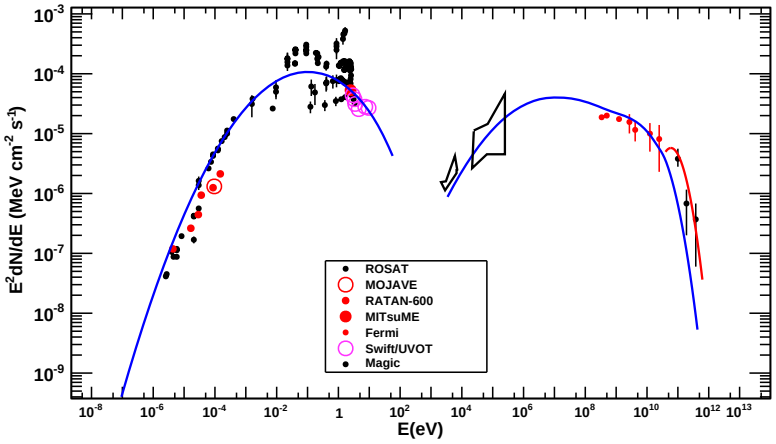

Fig. 1.— Fitting of observed spectral energy distribution (SED) of NGC1275. The blue line is a fit to the broadband SED using Fermi data, while the red curve is the pγ emission described in section 3.

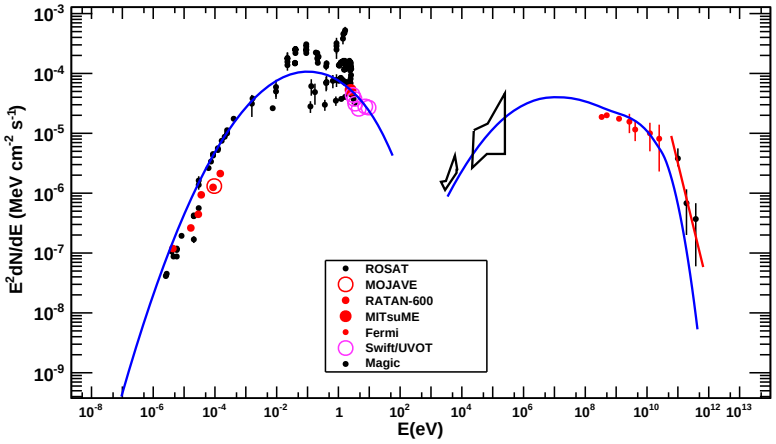

Fig. 2.— Fitting of observed spectral energy distribution (SED) of NGC1275. The blue line is a fit to the broadband SED using Fermi data, while the red curve is the pp emission described in section 3.

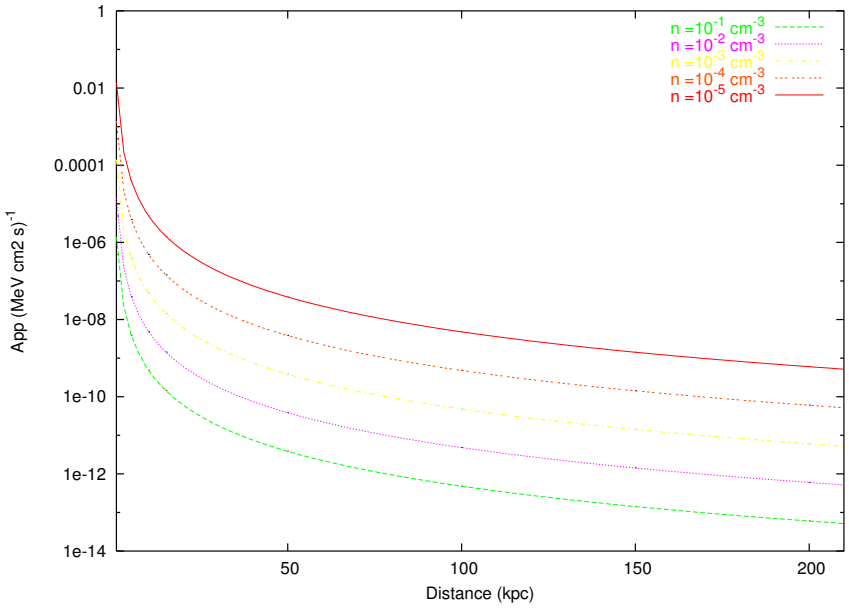

Fig. 3.— App as a function of the Lobes distance for several thermal particle densities for NGC1275